Tunable Mid-infrared $ZnGeP_2$ RISTRA OPO pumped by periodically-poled Rb:KTP optical parametric master-oscillator power amplifier

G. Stoeppler,[1,*] N. Thilmann,[2] V. Pasiskevicius,[2] A. Zukauskas,[2] C. Canalias,[2] and M. Eichhorn[1]

[1]*French–German Research Institute of Saint Louis ISL, 5 rue du Général Cassagnou, 68301 Saint-Louis, France*
[2]*Department of Applied Physics, Royal Institute of Technology, Roslagstullsbacken 21,10691 Stockholm, Sweden*
[*]*georg.stoeppler@isl.eu*

Abstract: A laser-diode pumped Q-switched single-frequency Nd:YAG MOPA operating at 100 Hz was used to generate tunable mid-infrared radiation between 6.27 µm and 8.12 µm by employing a cascaded parametric arrangement consisting of degenerate parametric master-oscillator power amplifier using a large aperture periodically-poled Rb:$KTiOPO_4$ which in turn pumped a $ZnGeP_2$ (ZGP) nonplanar RISTRA OPO. The noncollinear ZGP RISTRA tuning behavior is elucidated. The device is aimed for minimally invasive surgery applications at 6.45 µm where the peak power of 193 kW in 5 ns pulses is demonstrated.

OCIS codes: (190.4970) Parametric oscillators and amplifiers; (190.4360) Nonlinear optics, devices.

References and links

1. M. Lukac, T. Perhavec, K. Nemes, and U. Ahcan, "Ablation and thermal depths in VSP Er:YAG laser skin resurfacing," J. Laser Health Acad. **2010**, 56–71 (2010).
2. W. B. Telfair, C. Bekker, H. J. Hoffman, P. R. Yoder, Jr., R. E. Nordquist, R. A. Eiferman, and H. H. Zenzie, "Histological comparison of corneal ablation with Er:YAG laser, Nd:YAG optical parametric oscillator, and excimer laser," J. Refract. Surg. **16**(1), 40–50 (2000).
3. H. J. Hoffman and W. B. Telfair, "Photospallation: a new theory and mechanism for mid-infrared corneal ablations," J. Refract. Surg. **16**(1), 90–94 (2000).
4. G. S. Edwards, R. H. Austin, F. E. Carroll, M. L. Copeland, M. E. Couprie, W. E. Gabella, R. F. Haglund, B. A. Hooper, M. S. Hutson, E. D. Jansen, K. M. Joos, D. P. Kiehart, I. Lindau, J. Miao, H. S. Pratisto, J. H. Shen, Y. Tokutake, A. F. G. van der Meer, and A. Xie, "Free-electron-laser-based biophysical and biome-dical instrumentation," Rev. Sci. Instrum. **74**(7), 3207–3245 (2003).
5. M. S. Hutson and G. S. Edwards, "Advances in the physical understanding of laser surgery at 6.45 microns," 26th International Free Electron Laser Conference and 11th FEL User Workshop, pp. 648–653 (2004).
6. K. M. Joos, J. H. Shen, D. J. Shetlar, and V. A. Casagrande, "Optic nerve sheath fenestration with a novel wavelength produced by the free electron laser (FEL)," Lasers Surg. Med. **27**(3), 191–205 (2000).
7. M. A. Mackanos, D. Simanovskii, K. M. Joos, H. A. Schwettman, and E. D. Jansen, "Mid infrared optical parametric oscillator as a viable alternative to tissue ablation with the free electron laser," Lasers Surg. Med. **39**(3), 230–236 (2007).
8. K. L. Vodopyanov, F. Ganikhanov, J. P. Maffetone, I. Zwieback, and W. Ruderman, "$ZnGeP_2$ optical parametric oscillator with 3.8-12.4-mum tunability," Opt. Lett. **25**(11), 841–843 (2000).
9. A. Dergachev, D. Armstrong, A. Smith, T. Drake, and M. Dubois, "3.4-mum ZGP RISTRA nanosecond optical parametric oscillator pumped by a 2.05-mum Ho:YLF MOPA system," Opt. Express **15**(22), 14404–14413 (2007).
10. A. Dergachev, P. F. Moulton, and T. E. Drake, "High-power, high-energy Ho:YLF laser pumped by Tm:fiber laser " in Advanced Solid-State Photonics (ASSP)," OSA Trends in Optics and Photonics **98**, 608–612 (2005) (Optical Society of America).
11. M. Henriksson, M. Tiihonen, V. Pasiskevicius, and F. Laurell, "Mid-infrared ZGP OPO pumped by near-degenerate narrowband type-I PPKTP parametric oscillator," Appl. Phys. B **88**(1), 37–41 (2007).
12. M. W. Haakestad, G. Arisholm, E. Lippert, S. Nicolas, G. Rustad, and K. Stenersen, "High-pulse-energy 8 µm laser source based on optical parametric amplification in $ZnGeP_2$," Proc. SPIE **6998**, 699812, 699812-7 (2008).

#161046 - $15.00 USD Received 5 Jan 2012; revised 30 Jan 2012; accepted 30 Jan 2012; published 8 Feb 2012

13. A. Zukauskas, N. Thilmann, V. Pasiskevicius, F. Laurell, and C. Canalias, "5 mm thick periodically poled Rb-doped KTP for high energy optical parametric frequency conversion," Opt. Mater. Express **1**(2), 201–206 (2011).
14. M. A. Mackanos, E. D. Jansen, B. L. Shaw, J. S. Sanghera, I. Aggarwal, and A. Katzir, "Delivery of midinfrared (6 to 7-microm) laser radiation in a liquid environment using infrared-transmitting optical fibers," J. Biomed. Opt. **8**(4), 583–593 (2003).
15. D. J. Armstrong and A. V. Smith, "Demonstration of improved beam quality in an image-rotating optical parametric oscillator," Opt. Lett. **27**(1), 40–42 (2002).
16. A. V. Smith and D. J. Armstrong, "Generation of vortex beams by an image-rotating optical parametric oscillator," Opt. Express **11**(8), 868–873 (2003).
17. A. V. Smith and D. J. Armstrong, "Nanosecond optical parametric oscillator with 90° image rotation: design and performance," J. Opt. Soc. Am. B **19**(8), 1801–1814 (2002).
18. M. Henriksson, L. Sjöqvist, V. Pasiskevicius, and F. Laurell, "Mode spectrum of multi-longitudinal mode pumped near-degenerate OPOs with volume Bragg grating output couplers," Opt. Express **17**(20), 17582–17589 (2009).
19. D. E. Zelmon, E. A. Hanning, and P. G. Schunemann, "Refractive-index measurements and Sellmeier coefficients for zinc germanium phosphide from 2 to 9 μm with implications for phase matching in optical frequency-conversion devices," J. Opt. Soc. Am. B **18**(9), 1307–1310 (2001).
20. S. Brosnan and R. Byer, "Optical parametric oscillator threshold and linewidth studies," IEEE J. Quantum Electron. **15**(6), 415–431 (1979).

1. Introduction

Standard laser sources used in surgical applications exploit rapid buildup of the water vapour pressure with resulting fast expansion of the laser-heated volume to produce tissue ablation. Usually, such lasers operate at the 2 μm or 3 μm water absorption bands. Transitions in Tm^{3+} and Ho^{3+} around 2 μm and Er^{3+} at 2.94 μm employed in free-running or Q-switched lasers are almost exclusively used nowadays in surgery with exception of surgery on neural tissues and refractive surgery. Relatively long pulses, exceeding tens of nanoseconds, produced by such lasers, coupled with the tissue ablation threshold fluence for such pulses of above 1 J/cm^2, tends to produce relatively large thermal damage zones which are unacceptable in more delicate surgery, e.g., in brain or refractive eye surgery [1]. Interestingly, investigation of refractive surgery using pulses at 2.94 μm with different pulse lengths revealed that for the pulses with duration below 10 ns and having a short rise-time such as those generated by optical parametric oscillators (OPOs), the ablation threshold is reduced by an order of magnitude and the corneal ablation can be performed with submicron precision and with low collateral damage. The surgery results was very similar to those achieved using excimer lasers but without concomitant mutagenic risk [2]. It was proposed that this low threshold and high-precision ablation is possible due to so called photospallation mechanism [3]. With the aim of minimally invasive surgery, investigations were performed on tissue ablation in longer-wavelength mid-infrared range, 6.1 μm - 6.45 μm, where liquid water absorption band has varying overlap with amide-I and amide-II vibration bands in proteins [4–6]. These tissue ablation experiments using radiation from free-electron-lasers (FEL) revealed that the collateral damage effect was reduced and the healing of the target tissue was enhanced [4–6].

Obviously, an FEL is not a viable laser source for clinical surgery applications due to associated high costs. Moreover, its specific macropulse structure might not be the best suited for tissue ablation. Recent investigations have shown that an OPO with 100 ns pulses in the 6.1 μm - 6.45 μm range gave superior tissue ablation results in terms of lower thermal damage and larger ablation depth [7]. This particular $ZnGeP_2$ (ZGP) OPO was pumped by a Q-switched Er:YAG laser operating at 2.94 μm and the maximum output pulse energy was 250 μJ. For minimization of collateral thermal damage it is preferred to apply pulses shorter than the characteristic thermal confinement time (400 ns in cornea at 6.1 μm [7]) for reducing collateral thermal damage, but longer than the characteristic stress confinement time (3.1 ns in cornea at 6.1 μm [7]) in order to reduce detrimental effects of acoustic shock waves [3].

Our goal in this work was generating sub-10 ns, mJ-energy-level, tunable optical pulses in the 6 μm region with a high spatial beam quality. A ZGP OPO pumped at 2 μm is so far the most feasible solution for generating such pulses. ZGP crystals are characterized by high

#161046 - $15.00 USD Received 5 Jan 2012; revised 30 Jan 2012; accepted 30 Jan 2012; published 8 Feb 2012

nonlinear coefficient and low losses in the region between 2 μm and 8 μm, and, importantly, they are commercially available with large enough optical apertures [8].

One possible pump source for ZGP OPOs is a laser containing Ho^{3+}-doped host material which can emit above 2 μm while pumped by a Tm^{3+}-doped laser [9, 10]. Another pumping solution uses a cascaded pump scheme where a standard 1 μm Q-switched laser pumps a degenerate or close to degenerate OPO at 2 μm which, in turn, is used for pumping the ZGP OPO [11, 12].

The former pumping scheme can offer better overall system efficiency owing to the efficient diode pumping of Tm-lasers and low quantum defect of Ho^{3+}-laser. However, Q-switched Ho^{3+} lasers with the parameters required for the purposes of this work, namely, the pulse length shorter than 10 ns and pulse energies of tens of mJ and the repetition rate of at least 100 Hz are simply not available. Therefore in this work we chose the cascaded parametric scheme exploiting commercially available diode-pumped Q-switched single-frequency Nd:YAG maser-oscillator power amplifier as a pump source. In order to maximize the efficiency of the cascaded scheme we exploit recently developed large-aperture periodically poled $Rb:KTiOPO_4$ (PPRKTP) crystals [13] in the first step of the cascade. The requirements for beam quality are determined by the most desirable beam delivery method via mid-infrared solid-core fiber. The solid-core fibers suitable for the 6 μm - 7 μm region (chalchogenide and silver halide) have typical core diameters of larger than 300 μm in order to deliver the energies required for tissue ablation [14]. For launching a beam with high efficiency into such multimode fibers the low beam propagation factor, M^2, is not very critical, but the circular symmetry and low astigmatism of the beam are important. Achieving good beam quality in the idler beams in mid-infrared optical parametric oscillators is notoriously difficult.

A very promising technique to enhance the beam quality in the parametric process was proposed in [15] where the fact that the generated beam quality in critically phase-matched nonlinear interactions is much better in the direction of the Poynting vector walk off than in the orthogonal direction. This fact was exploited in a "Rotated Image Singly-Resonant Twisted RectAngle" (RISTRA) compact ring cavity arrangement where the image is rotated 90° either with a dove-prism or a 3-dimensional mirror arrangement, while the polarization of the resonant signal is restored by an intracavity half-wave plate [16, 17]. Such an arrangement eliminates beam astigmatism, increases the beam quality and allows a more efficient utilization of the nonlinear gain volume, determined by a circularly symmetric pump beam. This, in fact, reduces the RISTRA OPO threshold as compared to linear cavity designs. Owing to these important advantages we designed and built a tunable RISTRA ZGP OPO cavity for the second step of the cascaded parametric source.

2. Experimental setup

The schematic of the experimental setup is shown in Fig. 1. The pump laser was a diode-pumped Q-switched single-frequency (seeded with a DFB fiber laser) Nd:YAG delivering 80 mJ, 10 ns - long linearly polarized pulses at 1064.4 nm with a repetition rate of 100 Hz. The laser output was split by a thin-film polarizer P1 into two channels, one powering the master PPKTP OPO, while the other was used to pump a PPRKTP optical parametric amplifier (OPA). The powers in both pump arms could be adjusted by half-wave plate and thin-film polarizer (P2, P3) arrangements. The splitting ratio was controlled by a half-wave plate in the pump laser assembly.

The PPKTP OPO is operating at degeneracy and emits a wavelength of 2.128 μm which is wavelength stabilized by a volume Bragg grating (VBG) similar to that reported in Ref. 18.

#161046 - $15.00 USD Received 5 Jan 2012; revised 30 Jan 2012; accepted 30 Jan 2012; published 8 Feb 2012

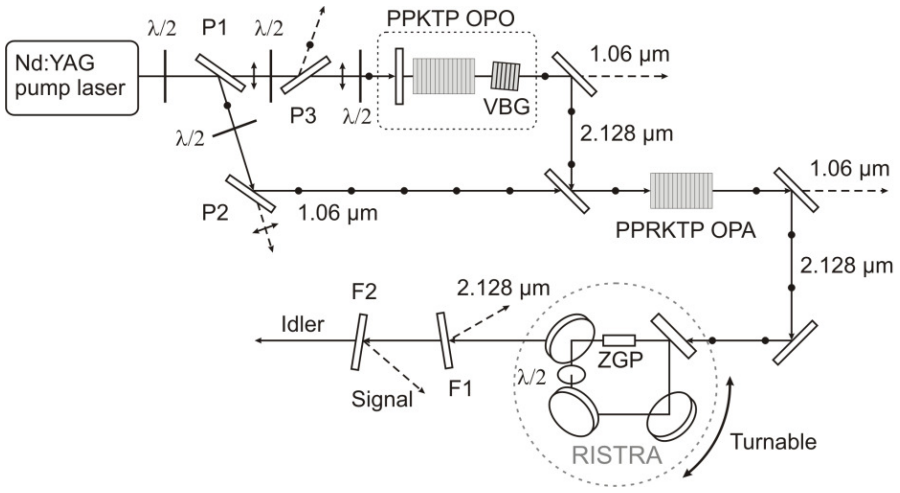

Fig. 1. Schematic drawing of the cascaded PPKTP OPMOPA stage and the ZGP RISTRA OPO.

The 6.45 μm radiation is generated using a ZGP OPO which has to be pumped with rather narrow-band spectrum at 2.128 μm to maximize the OPO efficiency [18]. We employed optical parametric master-oscillator power amplifier configuration for the 2.128 μm step of the cascade. Such configuration is less efficient than a single-OPO stage, but allows for better control over the beam quality and the spectral width of the output. This is especially important for relatively short and high-energy pulses where large Fresnel number OPO cavities have to be used. Due to the fact that the parametric gain bandwidth of degenerate type-I interaction in PPRKTP operating at 2.128 μm is very broad, of the order of 100 nm, the bandwidth narrowing in the first step of the cascade is mandatory. For narrowing the bandwidth at degeneracy, we employed a volume Bragg grating (VBG) with a reflectivity of 50% and FWHM reflectivity bandwidth of 0.5 nm as an output coupler in the PPKTP master OPO. The OPO contained 10 mm-long PPKTP with an optical aperture of 3 mm × 5 mm and with a ferroelectric domain period of 38.86 μm and it was pumped through a plane-plane incoupling mirror which was highly reflective at 2.128 μm while highly transmitting at the pump wavelength. The PPKTP OPO pump power was determined by two, generally opposing, requirements, i.e., the requirement of high enough output energy in order to efficiently extract the pump energy in the OPA stage, which means running the parametric amplifier in saturation regime and, at the same time, limiting the master OPO pumping level in order to maintain good beam quality. The beam quality can deteriorate quite drastically in a linear OPO cavity with large Fresnel number when the OPO is driven more than two-times above the oscillation threshold. The reason for this is cascaded upconversion and downconversion cycles in the nonlinear OPO medium, which produces intensity-dependent spatial phase shifts, akin to the B-integral in ultrashort-pulse laser amplifiers. For power amplification at 2.128 μm we employed a single-pass OPA containing a 16 mm-long PPRKTP crystal with the same domain period as the one in the OPO but with the optical aperture of 5 mm × 5 mm in order to accommodate the pump beam with a diameter of about 3 mm. Both PPRKTP crystals in the OPO and in the OPA as well as VBG were AR-coated for the pump and the parametric waves. The beam sizes of the OPA pump and the seed were matched using a telescope in the OPA pumping arm.

3. Experimental results and discussion

The PPKTP master OPO, VBG-locked at 2.128 μm, generated 3.6 mJ, 8 ns pulses two-times above the oscillation threshold. This was chosen as the operation point for the master OPO due to the above-mentioned tradeoffs. The master OPO beam was superimposed on the

#161046 - $15.00 USD Received 5 Jan 2012; revised 30 Jan 2012; accepted 30 Jan 2012; published 8 Feb 2012

dichroic mirror just before the PPRKTP OPA stage. The OPA was pumped with 60 mJ pulses at 1.064 µm.

For seeding the OPA stage we used 3.6 mJ pulse energy from the OPO with the pulse length of about 8 ns. At the maximum available pump energy of 60 mJ the OPA generated 26 mJ giving the amplification factor of 7.2 and the energy extraction efficiency of 43%. The output energy dependence on the pump pulse energy for the 2 µm MOPA is shown in Fig. 2.

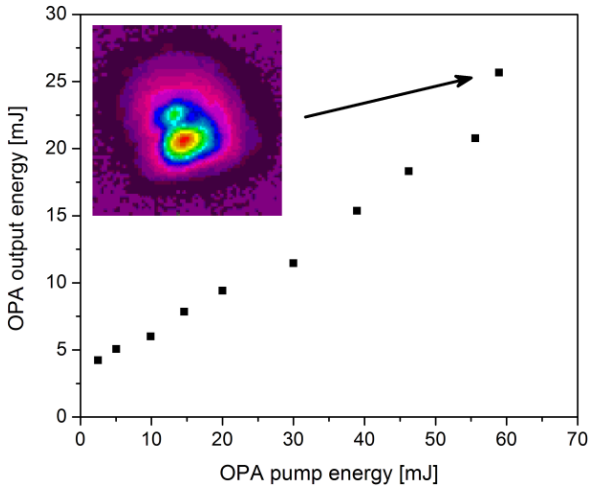

Fig. 2. Output energy of the 2.128 µm MOPA as a function of pump energy. Inset: output intensity profile of the MOPA.

The inset in Fig. 2 shows the MOPA output beam profile at maximum pump power. The intensity modulation apparent in the beam occurs due to spatial pulse front tilt introduced by the astigmatism-compensating arrangement in the OPA pump beam. Due to the fact that both the 2.128 µm master OPO and the power OPA operate at degeneracy and are coherently related to each other by being pumped by the same source the phase-sensitive nature of the parametric amplification transfers the spatial phase modulation of the pump onto the intensity modulation of the MOPA output. A simple method for avoiding such modulation is by using a single astigmatism compensation scheme for both the OPO and the OPA. On the other hand, the remnant intensity modulation in the 2 µm beam proved to be not detrimental for the beam quality of 6.45 µm OPO due to the properties of the RISTRA cavity. Owing to high energy stability of the laser diode pumping of the 1.064 µm Nd:YAG MOPA and the saturated operation of the parametric amplifier the energy stability of the 2.128 µm output was similar to that of the pump, namely pulse-to-pulse energy variations were about 1%.

The measured signal and idler output energies as a function of the 2.128 µm energy after the RISTRA incoupling mirror are shown in Fig. 3. For collinear alignment (the pump parallel to the resonated signal) the RISTRA generated 6.27 µm idler and 3.22 µm signal with corresponding maximum pulse energies of 0.84 mJ and 1.25 mJ, respectively (Fig. 3(a)). The RISTRA design allowed output wavelength tuning by simply rotating the cavity without any additional adjustments. For ± 1-degree rotation from the collinear position the idler tuned between 6.27 µm and 8.12 µm with the corresponding signal tuning between 3.22 µm and 2.88 µm.

#161046 - $15.00 USD Received 5 Jan 2012; revised 30 Jan 2012; accepted 30 Jan 2012; published 8 Feb 2012

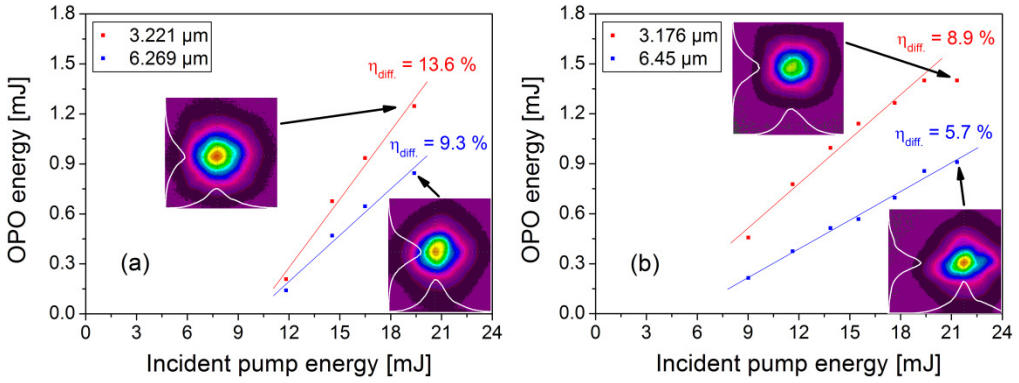

Fig. 3. Pulse energy of the signal and idler wavelength for collinear (a) and noncollinear (b) phase-matching with the intensity profile at maximum incident pump energy.

The noncollinear RISTRA performance corresponding to the idler at 6.45 μm, coinciding with the amide-II absorption band of interest for the surgery applications, is shown in the Fig. 3(b). The idler energy here was 0.91 mJ while the signal reached 1.4 mJ at the pump energy of 21.3 mJ. The insets in Fig. 3 show the RISTRA signal and idler beam intensity profiles measured at maximum pump energy at a distance of ~47 cm from the ZGP crystal. In both, the collinear and noncollinear phase matching the beam profiles are smooth although some astigmatism appeared in the idler beam in noncollinear phase-matching configuration. Apparently the remnant intensity modulation in the 2.128 μm beam did not influence the beam quality of the ZGP RISTRA OPO owing to the image-rotating properties of the cavity.

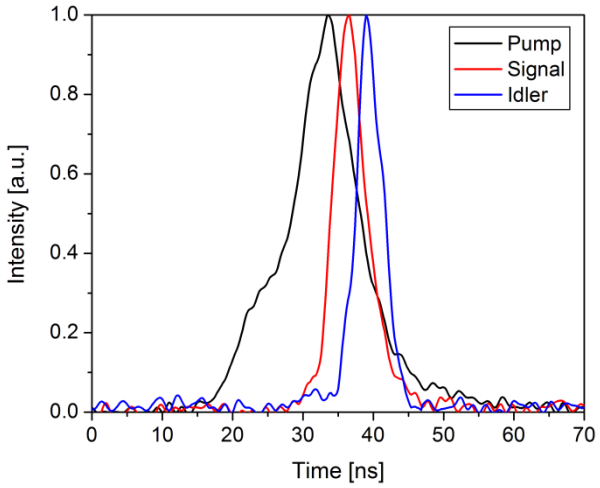

Fig. 4. The scaled pulse shape of the pump and the generated pulses from the ZGP RISTRA OPO with noncollinear phase matching at 3.17 μm and 6.45 μm.

We obtained a 4 mJ lower threshold with noncollinear phase matching but the slope of the idler decreased to 5.7%. The RISTRA cavity and the idler beam path were in ambient air. The ZGP RISTRA OPO generated 5 ns-long output pulses, corresponding to the idler peak power of 193 kW and the signal peak power of 230 kW. The pulses are displayed in Fig. 4 where the delay of the signal and idler pulse comes from different cable lengths.

The ZGP RISTRA OPO was tuned by rotating the cavity while the ZGP crystal was fixed with respect to the pump arrangement. Thereby the resonant signal direction with respect to the ZGP crystal c-axis was changed by rotating the cavity thus changing the pump-to-signal angle inside the crystal. The idler direction adjusted to satisfy momentum conservation

#161046 - $15.00 USD Received 5 Jan 2012; revised 30 Jan 2012; accepted 30 Jan 2012; published 8 Feb 2012

condition. The tuning behavior in such situation can be calculated from energy and momentum conservation by:

$$\omega_p = \omega_s + \omega_i \tag{1}$$

$$k_i^2 = k_p^2 + k_s^2 - 2k_p k_s \cos(\alpha_p) \tag{2}$$

Where in Eq. (1) and Eq. (2) ω_j, $j = p,s,i$ are corresponding pump, signal and idler frequencies, k_j are respective wave-vectors and α_p is the angle between the pump and signal. It is clear from Eq. (2), that the tuning is symmetric with respect to the rotation direction. This was indeed the case in the experiments.

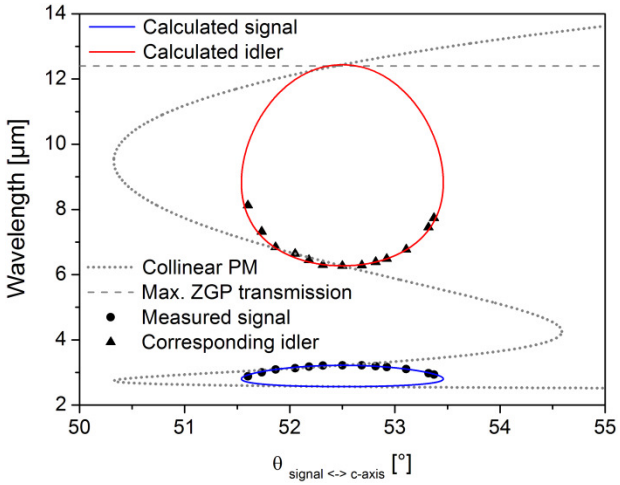

Fig. 5. Phase-matching curves for both type with the measured points and the calculated noncollinear phase-matching curves.

The calculated and measured tuning curves for the 52.5°-cut ZGP are shown in Fig. 5, where the measurement results are displayed by data points, while the dashed curve corresponds to the collinear phase matching and the solid curves show the noncollinear phase-matching. In these calculations we employed the Sellmeier expansion for ZGP given in Ref. 19. It is evident from Fig. 5 that the tuning in the collinear phase-matching case has characteristic retracing behaviour, therefore for the specific cut one could in principle be able to generate two signal-idler pairs. Due to such retracing behaviour, the noncollinear phase-matching is characterized by rather peculiar closed loops (solid curves in Fig. 5). In reality it would be difficult to cover the whole noncollinear tuning range due to limitations of the reflectivity range of the RISTRA OPO mirrors as shown by the experimental points in Fig. 5.

#161046 - $15.00 USD Received 5 Jan 2012; revised 30 Jan 2012; accepted 30 Jan 2012; published 8 Feb 2012

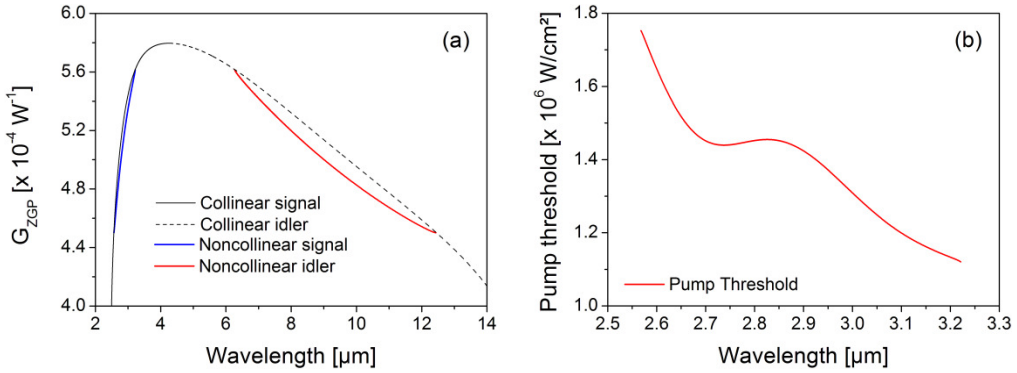

Fig. 6. Calculated parametric gain for the ZGP RISTRA OPO idler wavelength, (a) and the pump intensity at the ZGP OPO threshold as a function of the resonant signal wavelength, (b). In (a) slight gain decrease due to noncollinear phase-matching is evident.

In the experiment the ZGP RISTRA OPO idler could be tuned between 6.27 µm and 8.12 µm using noncollinear phase-matching by simply rotating the cavity without any additional adjustments. Moreover, while estimating the OPO threshold one has to account for the nonlinear coefficient variation with angle with respect to the ZGP c-axis and also noncollinear phase-matching angle. In the noncollinear configuration the gain is slightly lower due to lower noncollinear effective coefficient as shown in Fig. 6(a). In addition, high-reflectivity coatings have limited the spectral range. In calculating the ZGP RISTRA OPO threshold in Fig. 6(b) using the expression by Brosnan and Byer [20] we took into account both the noncollinear gain and the actual mirror reflectivity. These calculations clearly explain the limited experimental tuning range in Fig. 5. Actually, reaching the upper idler tuning branch would be rather difficult owing to lower gain and due to the ZGP linear transmission limit at 12.4 µm (indicated by the dashed horizontal line in Fig. 5).

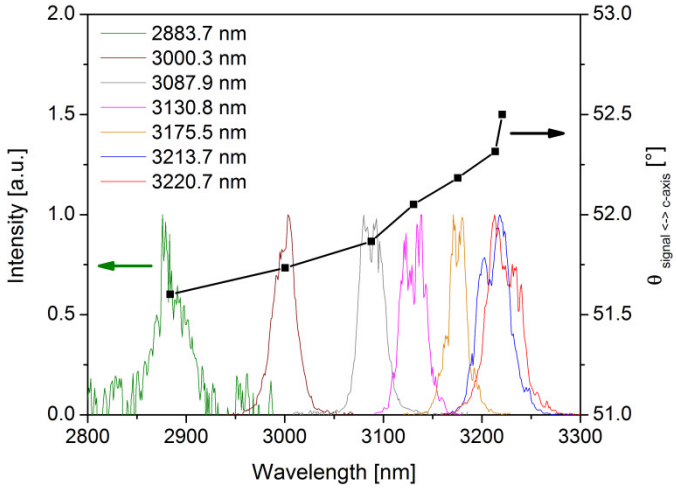

Fig. 7. The measured signal spectra ZGP RISTRA OPO tuned by counter-clockwise rotation of the cavity. The collinear phase-matching signal wavelength is 3.22 µm. For the clockwise rotation the signal spectra were identical. The corresponding range of idler wavelengths spans from 6.27 µm to 8.12 µm.

The measured signal spectra generated by rotating the RISTRA cavity are shown in Fig. 7. Here the RISTRA was rotated counter-clockwise, but as shown in Fig. 5 and as follows from Eq. (2), the tuning is symmetric for clock-wise rotation of the cavity. These spectra were used to determine the central wavelength by using a Gaussian fit and the values for the central

#161046 - $15.00 USD Received 5 Jan 2012; revised 30 Jan 2012; accepted 30 Jan 2012; published 8 Feb 2012

wavelengths were used in the phase-matching diagram in Fig. 5. The idler corresponding to the signal shown in Fig. 7 tunes between 6.27 µm and 8.12 µm. The average spectral width of the RISTRA OPO is about 750 GHz, a parameter which is not critical for the applications in laser-tissue interactions.

4. Summary and conclusion

We employed a commercially available diode-pumped Q-switched single-frequency Nd:YAG MOPA as a high-stability and high-energy pump source for a cascaded parametric scheme to obtain tunable radiation between 6.27 µm and 8.12 µm aimed at applications of minimally invasive surgery. The system operates at 100 Hz and produces 193 kW of peak power in 5 ns pulses at the wavelength of 6.45 µm where amide-II protein vibrational absorption bands overlap with the absorption band of liquid water. The cascaded system exploits large aperture PPRKTP crystals for parametric MOPA at degeneracy, VBG locking for spectral bandwidth narrowing at 2 µm and a ZGP OPO in nonplanar RISTRA configuration for high-spatial quality output beams generation in mid-infrared. The efficiency of the ZGP OPO is to large extent limited by relatively long RISTRA cavity and short pulse duration at 2 µm. Therefore, the rather low pulse energies used in a two crystal MOPA scheme could allow for higher efficiencies at a comparable beam quality, however under the expense of the need for two ZGP crystals and a more complex alignment than in case of a single RISTRA. Nevertheless, the generated energies are about four-times higher than the reported tissue ablation thresholds at 6.45 µm.

Acknowledgments

The research leading to these results has received funding from the European Community's seventh Framework Programme FP7/2007-2011 under grant agreement n° 224042.

#161046 - $15.00 USD Received 5 Jan 2012; revised 30 Jan 2012; accepted 30 Jan 2012; published 8 Feb 2012